Single-Step Formation of a Biorecognition Layer for Assaying Histidine-Tagged Proteins

Electra Gizeli*,† and Johanna Glad‡

Institute of Molecular Biology and Biotechnology, FORTH and Department of Biology, University of Crete, Vassilika Vouton, Heraklion, Crete, Greece 71110, and Institute of Biotechnology, University of Cambridge, Tennis Court Road, Cambridge, CB2 1QT, U.K.

The purpose of this work was to develop a simple procedure for the creation of a specific biorecognition layer for histidine-tagged (His-tagged) molecules. Such a layer was prepared by the spontaneous fusion of vesicles containing readily available plain (DOPC) and iminodiacetic acid (DOGS-NTA) phospholipids on a silica surface resulting in the formation of an NTA-containing supported lipid bilayer. The frequency surface acoustic waveguide device which supports Love waves was used to follow the real-time formation of the biorecognition layer. The mole percent of the DOGS-NTA phospholipids in the supported bilayer was optimized by following the kinetics of the fusion for the different NTA-containing lipids. Fluorescently labeled lipids were used with observations of the fluorescence recovery after photobleaching to confirm the presence of lipid bilayers. After saturating all NTA-molecules with Ni^{2+}, the binding of a His-tagged protein fragment within the concentration range of 0.04 and 0.4 mM to a 5 mol % DOGS-NTA/DOPC was detected; binding curves were used to calculate the apparent association constant $k_{on} = 2.56 \times 10^4\ M^{-1}\ s^{-1}$, dissociation constant $k_{off} = 1.3 \times 10^{-3}\ s^{-1}$, and equilibrium constant $k_{eq} = 1.97 \times 10^7\ M^{-1}$. The described method could find significant applications as a generic technique for preparing biorecognition layers for His-tagged proteins. In addition, the acoustic waveguide device, which provides high sensitivity together with flexibility in terms of the substrate material used, is shown to be an attractive alternative to direct optical biosensors.

The development of a specific biorecognition surface on a solid/liquid interface is of high significance in the areas of drug screening, proteomics, and biosensors. A primary challenge in developing such an interface is the design of a biorecognition layer that will possess the desirable properties of specificity, biocompatibility, and reversibility of the binding event. One method that has become instrumental for both the identification and purification of gene products is the immobilization of fusion proteins incorporating a polyhistidine tail. It is possible to engineer proteins, protein fragments, or peptides to obtain a short sequence of six adjacent histidine residues and, subsequently, immobilize them in an oriented manner on a solid support by using metal affinity chromatography techniques.[1] The immobilization of His-tagged proteins has been demonstrated on gold,[2−5] glass,[6] and polymer[7] surfaces in combination with self-assembled thiol molecules, silanes, and surfactants, respectively. All of the above approaches are laborious and time-consuming, requiring first, the synthesis of a metal chelating agent, which normally includes a nitrilotriacetic acid (NTA) or iminodiacetic acid (IDA) group; and second, the attachment of the chelating agent to the solid surface.

The binding of the His-tagged molecule to the solid surface has been studied using numerous techniques, including surface plasmon resonance (SPR),[2−5,8] total internal reflection fluorescence,[6] the resonant mirror,[9] bioluminescence,[7] X-ray photoelectron and correlation spectroscopy,[10] and atomic force microscopy (AFM).[5] The advantage of real-time techniques is that they can be used for the determination of the kinetic and equilibrium constants of the binding of the His-tagged molecule to the surface; the latter can be referred to as the apparent constants in order to distinguish them from the measurement of the same constants in solution. Acoustic devices[11] can also be used for the real-time measurement of the binding of a biomolecule to the device surface. The most popular devices include those based on the high-frequency shear surface acoustic wave (SAW) device, such as the acoustic waveguide and acoustic plate mode (APM), or the low-frequency bulk acoustic wave (BAW) device, such as the thickness shear mode (TSM) resonator, also known as the quartz crystal

* Corresponding author. E-mail: e.gizeli@imbb.forth.gr.
† University of Crete.
‡ University of Cambridge.

(1) Porath, J. *Protein Purif. Expression* **1992**, *3*, 263−281.
(2) Stora, T.; Dienes, Z.; Vogel, H.; Duschl, C. *Langmuir* **2000**, *16*, 5471−5478.
(3) Sigal, G. B.; Bamdad, C.; Barberis, A.; Strominger, J.; Whitesides, G. M. *Anal. Chem.* **1996**, *68*, 490−497.
(4) Keller, T. A.; Duschl, C.; Kroger, D.; Sevin-Landais, A.-F.; Vogel, H. *Supramo. Sci.* **1995**, *2*, 155−160.
(5) Raedler, U.; Mack, J.; Persika, N.; Jung, G.; Tampe, R. *Biophys. J.* **2000**, *79*, 3144−3152.
(6) Schmid, E.; Keller, T. A.; Dienes, Z.; Vogel, H. *Anal. Chem.* **1997**, *69*, 1979−1985.
(7) Ho, C.-H.; Limberis, L.; Caldwell, K. D.; Stewart, R. J. *Langmuir* **1998**, *14*, 3889−3894.
(8) Nieba, L.; Nieba-Axmann, S. E.; Persson, A.; Mamalainen, M.; Edebratt, F.; Hansson, A.; Lidholm, J.; Magnusson, K.; Frostell-Karlsson, A.; Plucthun, A. *Anal. Biochem.* **1997**, *252*, 2217−228.
(9) Altin, J. G.; White, F. A. J.; Easton, C. J. *Biochim. Biophys. Acta* **2001**, *1513*, 131−148.
(10) Davis, J.; Glidle, A.; Cass, A. E. G.; Zhang, J.; Cooper, M. J. *J. Am. Chem. Soc.* **1999**, *121*, 4302−4303.
(11) Ballantine, D. S.; White, R. M.; Martin, S. J.; Ricco, A. J.; Zellers, E. T.; Frye, G. C.; Wohltjen, H., Eds. *Acoustic Wave Sensors*; Academic Press: San Diego, 1997.

10.1021/ac034855g CCC: $27.50
Published on Web 00/00/0000

microbalance (QCM). Acoustic wave biosensors utilizing the acoustic waveguide geometry or the TSM resonator have been applied to the study of antibody−antigen, antibody−peptide and membrane-related interactions.[12−14] In addition, the TSM resonator has been used extensively to elucidate the mechanism of the formation of a supported lipid bilayer during the spontaneous fusion of vesicles with a hydrophilic surface.[15,16]

In this paper, we are introducing a general, simple, and robust approach for the reversible immobilization of histidine-tagged proteins on a hydrophilic surface, which eliminates the laborious requirement for multistep synthetic chemistries described in previous studies. Our approach, outlined in Figure 1a, was to develop a nickel-chelating supported lipid bilayer (SLB) on a solid support by simply fusing vesicles containing NTA lipids with a hydrophilic silica surface. Once a bilayer containing NTA lipids is deposited on the device surface, nickel can be used to chelate the NTA groups with proteins containing a histidine tail. This method ensures specific and oriented attachment of the protein of interest to the device surface, together with the ability to regenerate the surface. For the real-time monitoring of the binding events, we used the acoustic waveguide device (Figure 1b) that has been designed, developed, and successfully tested to sense mass changes occurring in biological layers deposited on the device surface.[17−19] A dielectric layer (silica in this application) deposited on the device surface serves as an acoustic waveguide by localizing acoustic energy onto the sensing surface and generating a Love wave. The presence of the waveguide layer on the 108-MHz acoustic device enhances the surface sensitivity to mass deposition by 35 times as comparing to the nonlayered structure.[20] High-frequency surface acoustic wave devices, such as the waveguide geometry, are known to exhibit significantly higher mass sensitivity than the lower-frequency quartz crystal microbalance.[11] Moreover, various materials can be used as a guiding layer, for example, gold, silica, or polymers, giving the flexibility to attach the biorecognition layer to the most appropriate substrate. When the device is in contact with an aqueous sample, then an acoustic evanescent wave is developed inside the liquid that extends ∼55 nm in the solution. The velocity of the wave, measured as phase, has been modeled and experimentally shown to be proportional to surface-attached mass.[11]

EXPERIMENTAL SECTION

Materials. 1,2-Dioleoyl-*sn*-glycero-3-phosphocholine (DOPC) and 1,2-dioleoyl-*sn*-glycero-3-{[*N*-(5-amino-1-carboxypentyl)imino-diacetic acid]succinyl} (DOGS-NTA) were obtained from Avanti Polar Lipids, Alabaster, AL; 2-(12-(7-nitrobenz-2-oxa-1,3-diazol-4-yl)amino)dodecanoyl-1-hexadecanoyl-*sn*-glycero-3-phosphocholine (NBD-C_{12}−HPC) was obtained from Molecular Probes Europe; and $NiSO_4$, EDTA, Triton X-100, immunoglobulin G (IgG), bovine serum albumin (BSA), and phosphate buffer saline (PBS) tablets (0.01 M phosphate, 0.0027 M KCl, and 0.137 M NaCl, pH 7.4) were obtained from Sigma.

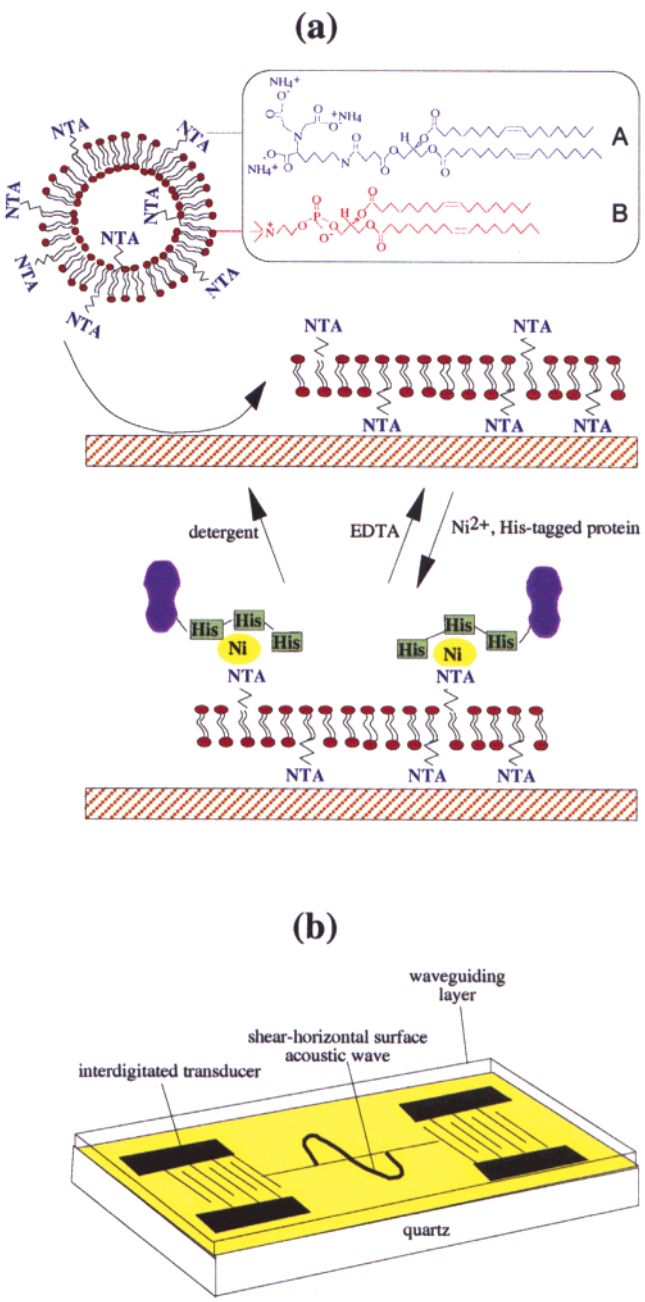

Figure 1. (a) Vesicles containing DOGS-NTA (A) and DOPC (B) lipids were fused on a silica surface to form a supported lipid bilayer; the latter was further applied for the binding of a His-tagged protein after addition of Ni^{2+}. The regeneration of the silica or NTA-lipid-bilayer surface was achieved after washing with detergent or EDTA, respectively. (b) Acoustic waveguide geometry: a surface acoustic wave device operating at 108 MHz was used to generate a shear horizontal wave by applying an electric potential via the interdigitated transducers. A silica layer (2.4 μm) deposited on the device surface was used as a waveguiding layer.

Acoustic Devices. The acoustic devices were prepared by photolithography at the Southampton Electronics Center (Southampton, U.K.) using single-crystal Y-cut, z-propagating, 0.5-mm-thick

(12) Cavic, B. A.; Hayward, G. L.; Thompson, M. *Analyst* **1999**, 1405−1420.
(13) Janshoff, A.; Galla, H.-J.; Steinem, C. *Angew. Chem. Int. Ed.* **2000**, *39*, 4004−4032.
(14) Gizeli, E. In *Biomolecular Sensors*; Gizeli, E., Lowe, C. R., Eds.; Taylor and Francis: London, 2002; pp 176−207.
(15) Keller, C. A.; Kasemo, B. *Biophys. J.* **1998**, *75*, 1397−1402.
(16) Reimhult, E.; Hook, F.; Kasemo, B. *Langmuir* **2003**, *19*, 1681−1691.
(17) Gizeli, E.; Stevenson, A. C.; Goddard, N. J.; Lowe, C. R. *IEEE Trans. Ultrason. Ferroelectr. Frequency Control* **1992**, *39*, 657−659.
(18) Gizeli, E.; Liley, M.; Lowe, C. R.; Vogel, H. *Anal. Chem.* **1997**, *69*, 4808−4813.
(19) Harding, G.; Du, J.; Dencher, P.; Barnett, D.; Howe, E. *Sens. Actuators, A* **1997**, *61*, 279−286.
(20) Gizeli, E.; Stevenson, A. C.; Goddard, N. J.; Lowe, C. R. *Sens. Actuators, B* **1993**, *14*, 638−639.

quartz with a 200-nm gold overlayer and a 10-nm chromium adhesion layer. The input and output interdigitated transducers (IDTs) produced by the photolithographic patterning consisted of 80 pairs of split fingers with a periodicity of 45 μm; the wavelength of the acoustic wave was therefore 45 μm, and the operating frequency of the uncoated device was 108 MHz.

Waveguide Geometry. A silica layer of 2.4 μm was deposited directly onto the device surface by plasma-enhanced chemical vapor deposition (CVD), using a capacitively coupled system (Oxford Instruments DP80) operating at a frequency of 13.56 MHz. Mixtures of gas containing SiH_4, N_2O, and He were introduced to the reaction chamber at a pressure of 1000 mTorr. The substrate was heated to 350 °C during the deposition. Silica surfaces were used directly after silica deposition. Between experiments, the device was cleaned by sonication in 2% Hellmanex II (Hellma, Mullheim, Germany) solution for 10 min, followed by sonication in water for an additional 10 min and drying under a steam of nitrogen. The operating frequency of the silica-coated acoustic waveguide device was 104 MHz.

Instrumentation and Experimental Setup for Acoustic Experiments. A Hewlett-Packard 4195A network analyzer was used to measure the amplitude and phase of the output electrical signal with respect to a reference signal. Data were collected on a PC using LabView software. A Perspex flow cell with a silicone rubber gasket was used to hold the solution in place over the region of the device between the IDTs, exposing an area of ~0.12 cm^2. During experiments, a 3-MHz region of the frequency spectrum near the maximum operating frequency was scanned every 43 s to monitor the signal. Data were collected at a fixed frequency so that one data point was collected every 43 s. Experiments were carried out at ambient temperature (e.g., 23 °C).

Preparation of Lipid Vesicles. Unilamellar lipid vesicles containing DOPC and various mole ratios of DOGS-NTA were prepared by extrusion using an Avestin Liposofast Basic extrusion apparatus. Stock solutions of lipids were made up in chloroform and mixed to give the appropriate molar ratio. The chloroform was removed by evaporation under nitrogen for 1 h. The dried lipids were resuspended in PBS at a total lipid concentration of 2 mg/mL and then extruded 21 times through a 50-nm pore membrane (Avestin).

Acoustic Real-Time Experiments. A continuous flow of PBS was pumped over the surface of the acoustic device at a rate of 7 μL/min using a peristaltic pump. Vesicle suspensions at a concentration of 0.02 mg/mL total lipid content were run over the surface of the device for 15 min. The device was then rinsed with PBS until the acoustic signal had reached a steady state, followed by successive additions of 100 mM of $NiSO_4$; PBS; and finally, various concentrations of the His-tagged protein solution. Regeneration of the device and lipid surfaces was achieved by introducing 0.1% w/v Triton X-100 and 350 mM EDTA, respectively.

For the control experiments, 0.05 mg/mL of the histidine-tagged protein and IgG and BSA were applied on a DOPC and 5 mol % DOGS-NTA/DOPC-supported lipid bilayer, respectively, followed by a buffer rinse at a flow rate of 7 μL/min.

Fluorescence Microscopy. Vesicles containing 1, 2, 5, and 10 mol % DOGS-NTA/DOPC together with 0.1 mol % of the fluorescently labeled lipid NBD-C_{12}−HPC were applied to the device surface as described above. After monitoring the deposition of the lipid vesicles by following the acoustic response, devices were examined by fluorescence microscopy. A Nikon microscope equipped with a B-2A filter block (λ_{ex} 450−490 nm; λ_{em} > 505 nm) was used. A small spot on the sample was illuminated with the UV source and left to bleach; after this, it was left in the dark for 10−15 min before being photographed.

RESULTS

Formation of a Supported Lipid Bilayer Containing NTA Lipids. Vesicle suspensions containing different molar ratios of DOGS-NTA/DOPC lipids were prepared and applied to the silica surface. Figure 2a shows the acoustic wave response in real time for vesicles containing 1, 2, 5, and 10 mol % DOGS-NTA. For the first three suspensions, the signal decreases and finally equilibrates after reaching a minimum phase value. The time it takes to equilibrate is $t_1 = 170$ s for the 1 mol % and $t_1 = 270$ s for the 2 and 5 mol % DOGS-NTA suspensions. In the case of the 10 mol % suspension, the signal decreases monotonically and within the time period of the experiment does not reach equilibrium.

After applying the vesicle suspension on the device surface and performing the acoustic experiments, devices were transferred and checked under the microscope while keeping their surface continuously in contact with water. Figure 2b shows three photographs of an area of ~0.02 mm^2 of a device surface preexposed to 5 mol % of DOGS-NTA/DOPC vesicles. The photographs taken were, from left to right: (i) just before the area was exposed to the UV source, (ii) immediately after it was exposed and bleached for few minutes, and (iii) after the shutter was closed and the surface was left in the dark for 10 min. The recovery of the initial intensity in the last photograph indicates that a fluid bilayer was formed on the device surface where the lipids exhibit lateral mobility.

Detection of His-Tagged Molecules. Histidine-tagged proteins were bound to the NTA-containing SLB after saturating all NTA sites with nickel by exposing the surface to 100 mM of $NiSO_4$. In this experiment, a His-tagged antibody fragment of a molecular weight of 12 500 Da was used to bind to the Ni-exposed surface. Figure 3 shows the phase change observed on addition of 0.3 μM of the His-tagged antibody as a function of the mol % of DOGS-NTA lipids used in the vesicle suspension. Figure 4 shows the normalized phase change recorded after the application of 0.04−0.4 μM solutions of the His-tagged protein on a SLB formed from a vesicle suspension containing 5 mol % DOGS-NTA lipids. Each protein concentration was measured on a fresh SLB after regenerating the device surface.

Figure 5a shows the real-time binding curves of the various concentrations of the His-tagged protein fragment to the 5 mol % DOGS-NTA/DOPC bilayer. These curves were used to calculate the apparent kinetic constants of the protein binding to nickel after fitting the data to a single exponential. Plotting the change of the slope divided by the maximum phase change, that is, $\Delta(dP/dt)/(\Delta P)$, as measured from Figure 5a, against the protein concentration gives a straight line with a slope that corresponds to the association rate constant (k_{on}) of the binding and an intercept with the y axis that corresponds to the dissociation rate constant (k_{off}) (Figure 5b).

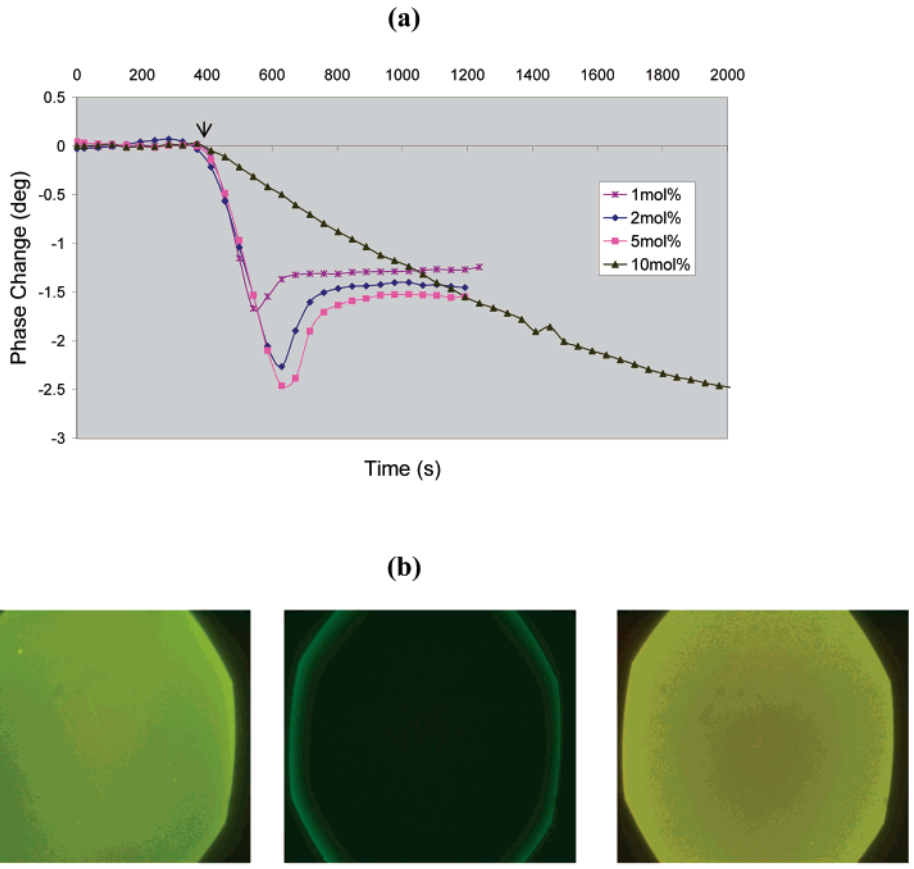

Figure 2. (a) Acoustic detection of the interaction of DOGS-NTA/DOPC vesicles with silica. Vesicles of DOPC containing 1, 2, and 5 mol % DOGS-NTA initially adsorb on the device surface (signal decrease) prior to fusion (signal increase) and final formation of a supported lipid bilayer (signal stabilization); vesicles containing more than 10 mol % DOGS-NTA adsorb onto the surface but stay intact and do not fuse. (b) Recovery of photobleaching of a supported lipid bilayer containing 5 mol % DOGS-NTA/DOPC lipids and 0.1 mol % NBD-DPHE. Photographs were taken from left to right: before, during, and 10 min after photobleaching.

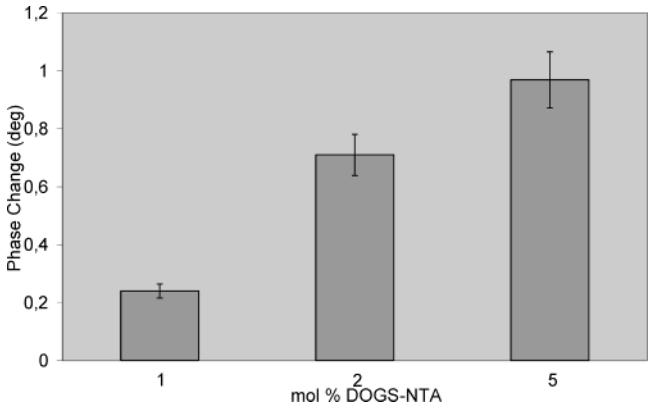

Figure 3. Histogram of the acoustic wave response obtained on application of 0.3 μM of a His-tagged protein to a Ni-exposed SLB containing 1, 2, and 5 mol % of DOGS-NTA/DOPC lipids.

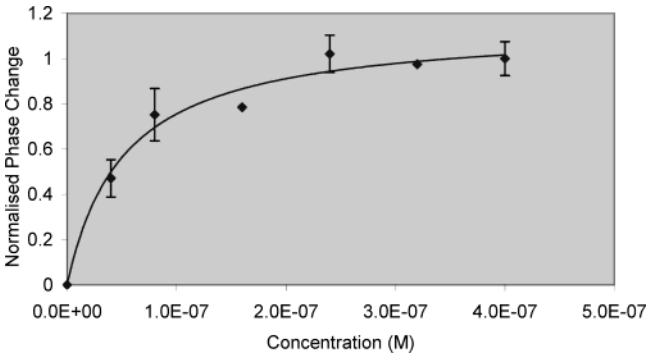

Figure 4. Binding isotherm of the His-tagged antibody fragment to the 5 mol % DOGS-NTA/DOPC supported lipid bilayer after the latter has been exposed to a concentrated solution of nickel. The solid line was calculated after fitting the experimental data to a Langmuir isotherm.

Figure 6 shows the course of a binding experiment involving the formation of a SLB from 5 mol % DOGS-NTA/DOPC vesicles, surface regeneration on addition of detergent (Triton or Hellmanex), and reformation of the same SLB, followed by nickel addition (100 mM), binding of 50 μg/mL of the His-fragment, lipid-surface regeneration on exposure to EDTA (350 mM), nickel reloading, and rebinding of 50 μg/mL of the His-fragment.

DISCUSSION

Vesicle Fusion as a Method for Forming NTA-Supported Lipid Bilayers; Optimization of the Amount of NTA Lipids. The successful formation of a homogeneous NTA-containing SLB is critical for developing a biorecogniton layer that binds specifically His-tagged molecules. Supported lipid bilayers containing NTA lipids were formed during the spontaneous fusion of vesicles on a silica surface. This procedure is simple and results in a lipid bilayer that maintains fluidity. Fused SLBs have been used extensively for developing planar bilayers in an array format.[21] The mechanism of the formation of a SLB has been studied

(21) Groves, J. T.; Ulman, N.; Boxer, S. G. *Science* **1997**, *275*, 651−653.

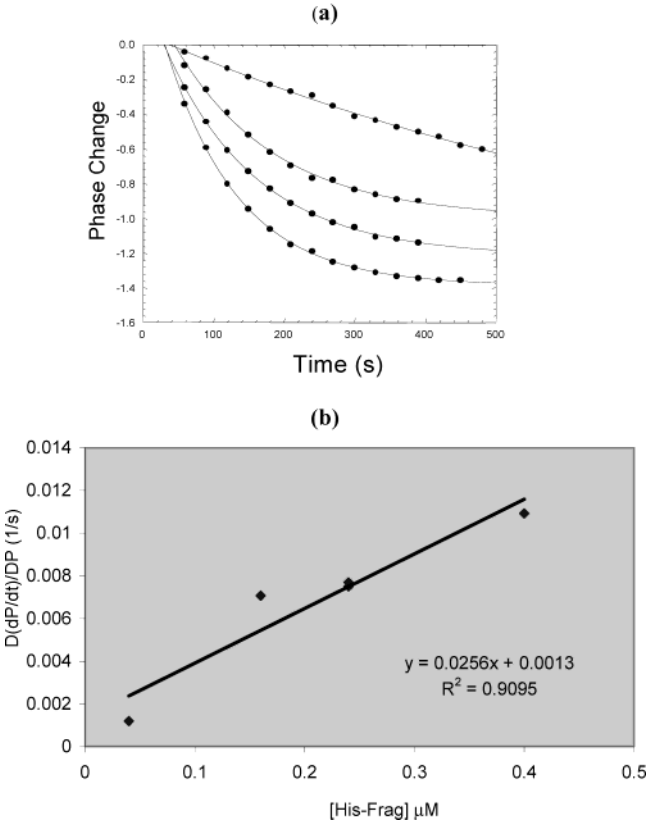

Figure 5. (a) Real-time binding curves of various concentrations of the His-tagged protein fragment to a 5 mol % DOGS-NTA/DOPC bilayer. The solid lines represent single-exponential fits to the data; (b) Calculation of the apparent kinetic constants of the His-tagged protein binding to nickel. The *y* axis was calculated from the real time plots shown in Figure 4a by measuring the change of the slope for each concentration of His-tagged protein that is, $\Delta(dP/dt)$, and then dividing it by the maximum phase change (ΔP) observed after signal saturation.

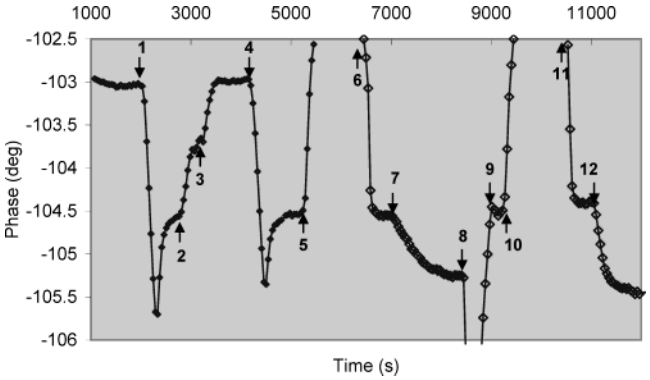

Figure 6. Real-time acoustic monitoring of the formation of a SLB from 5 mol % DOGS-NTA/DOPC vesicles (1); surface regeneration on addition of detergent (2) and buffer (3); reformation of the same SLB (4); nickel addition (5) and buffer rinse (6); binding of 50 μg/mL of the His-fragment (7); lipid-surface regeneration on exposure to EDTA (8) and buffer (9); nickel reloading (10) and buffer rinse (11); and rebinding of 50 μg/mL of the His fragment (12).

acoustically with the low-frequency (5-MHz) TSM resonator device and has been correlated to the vesicle size, surface chemistry, temperature, and osmotic pressure.[16,22−25] The effect of surface roughness has been also investigated with the high-frequency acoustic waveguide device during the fusion of vesicles with a hydrophilic silicate surface.[26] Understanding the mechanism of this interaction is crucial for sensing applications in order to ensure that a homogeneous SLB has been deposited on the device surface instead of a nonhomogeneous layer with many unfused vesicles or a vesicle layer.

The optimum amount of NTA lipids required for the formation of a SLB was investigated by monitoring the acoustic signal during the fusion of NTA-containing vesicles. Figure 2a shows the phase change monitored in real time during the application of 1, 2, 5, and 10 mol % DOGS-NTA/DOPC vesicles to the silica-coated acoustic waveguide device surface. Qualitatively, the shape of the acoustic signal detected during the fusion of the first three vesicle suspensions was found to be very similar and in accordance with the two-step kinetics reported in the literature that correspond to the formation of a SLB.[23] The first step involves the absorption of vesicles on the device surface and is attributed to attractive van der Waal forces between vesicles and the silica surface. Single vesicles deform after adsorption but do not rupture at low surface coverage; instead, they remain intact until a critical coverage is achieved at a time t_1. This step is detected in Figure 2 as a phase decrease with the minimum point corresponding to the surface when the maximum number of vesicles has been adsorbed. Once a critical deformation is achieved at a critical surface coverage, the second step starts, which involves rupture and fusion of vesicles, probably mediated by lateral interaction between neighboring vesicles, until a supported lipid bilayer is formed. The beginning of vesicle fusion is indicated in Figure 2 as phase increase, with the SLB being formed by the time the phase signal equilibrates. Quantitatively, the major difference between 1, 2, and 5 mol % is the time it takes to reach the minimum surface concentration, that is, t_1. One possible explanation is that the first step is associated mainly with the surface-vesicle interaction and that this interaction becomes weaker as the number of NTA lipids on the vesicle surface increases; consequently, a higher critical surface density is required to compensate for the decrease in the vesicles' deformation. This can be explained if one takes into account the negative nature of both silica and NTA molecules at the working pH of 7.4. The application of higher mole percent of DOGS-NTA resulted in stable vesicles that could adsorb onto the surface but were resistant against deformation and fusion. This behavior is shown in Figure 2 during the application of 10 mol % of DOGS-NTA vesicles. The above result is consistent with the observation that vesicles containing 10% of negatively charged lipids stabilize the spherical shape of the vesicles.[2] On the basis of Figure 2a, it appears that any of the three lower mole percents of DOGS-NTA/DOPC vesicles could be used for the formation of a SLB.

Acoustic information on the type of supported layer formed as a function of the mole percent of DOGS-NTA was further confirmed by using fluorescently labeled lipids and observing fluorescence recovery after photobleaching (FRAP). A homoge-

(22) Keller, C. A.; Kasemo, B. *Phys. Rev. Lett.* **2000**, *84*, 54434−55446.
(23) Keller, C. A.; Glasmaestar, K.; Zhdanov, V. P.; Kasemo, B. *Phys. Rev. Lett.* **2000**, *84*, 5443−5446.
(24) Reimhult, E.; Hook, F.; Kasemo, B. *Phys. Rev. E: Stat. Phys., Plasmas, Fluids, Relat. Interdiscip. Top.* **2002**, *66*, 051905 (1−4).
(25) Reimhult, E.; Hook, F.; Kasemo, B. *J. Chem. Phys.* **2002**, *117*, 7401−7404.
(26) Melzak, K.; Gizeli, E. *J. Colloid Interface Sci.ence* **2002**, *264*, 21−28.

neous supported lipid bilayer should maintain the dynamic properties of natural membranes and should, thus, exhibit the fluidity associated with natural membranes. The two-dimensional fluidity of SLBs containing 1, 2, and 5 mol % DOGS-NTA was confirmed by observing recovery of the fluorescence after photobleaching (Figure 2b). Fluorescent images did not reveal any adsorbed vesicles on the SLBs, even though the final phase change observed in Figure 2a suggests that slightly more mass has been deposited with the 2 and 5 mol % DOGS-NTA vesicles than with the 1 mol %. The formation of a supported vesicle layer when a vesicle suspension of 10 mol % DOGS-NTA was applied on the device surface was confirmed by observing no recovery of the fluorescence after photobleaching (data not shown).

The amount of protein binding to the different mole percents of NTA-containing SLB was also investigated. Results showed that the His-tagged protein bound to the device surface increased with increasing the mole percent of NTA lipids used during vesicle preparation, suggesting a correlation between the originally applied lipid ratios and the lipid composition in the supported bilayer (Figure 3). For the development of this biorecognition layer, vesicles containing 5 mol % DOGS-NTA were found to be a good compromise between having the maximum available number of nickel-chelating lipids and being able to form a SLB and were, therefore, applied in all further work.

Finally, the reproducibility of the formation of a SLB containing 5 mol % DOGS-NTA, as determined by the final acoustic signal change measured after applying the vesicle suspension and rinsing the surface with buffer, was investigated and found to be 98.4%. Deposited layers exhibited excellent chemical stability and could be removed only by detergent solutions. Addition of EDTA (0.05 mM) in the PBS buffer reduced the reproducibility of the bilayer formation to 80.5%, implying that the presence of metal impurities in the buffer is used to chelate the NTA molecules to the silica surface and stabilize the structure.

His-Tagged Protein Binding Isotherm; Measurement of Kinetic and Equilibrium Constants. Exposure of the DOPC/DOGS-NTA supported bilayer to nickel results in a surface that could bind specifically His-tagged molecules (Figure 1). Application of a His-tagged antibody fragment within the concentration range of 0.04−0.4 μM was detected acoustically by monitoring the phase of the wave. Figure 4 shows the binding isotherm of the His-tagged antibody to the NTA-bound nickel. Fitting the data to a Langmuir isotherm allowed the calculation of the apparent binding constant, which is equal to the inverse of the concentration at which one-half of maximal binding occurs; on the basis of Figure 4, k_{eq} was calculated to be 1.92×10^7 M^{-1}.

A more accurate way to obtain information about both the on and off rates of the antibody/Ni^{2+} binding and about the binding constant relies on the analysis of the real-time binding curve of each antibody concentration to the Ni^{2+} saturated NTA-SLB system.[27] For binding processes in which diffusion is not rate-determining, the binding kinetics can be described by the rate equation

$$dR/dt = k_{on}C_{Ab}(R_{max} - R) - k_{off}R$$

where R is the phase response of the device and is proportional to the amount of adsorbed antibody, C_{Ab} is the concentration of the His-tagged fragment in solution, k_{on} is the association rate constant, and k_{off} is the dissociation rate constant. Plotting (dR/dt) against R gives a straight line with a gradient of

$$\Delta(dR/dt)/\Delta R = k_{on}C_{IgG} + k_{off}$$

Plotting this gradient versus IgG concentration for the individual measurements at different concentrations, we should thus obtain a straight line with a gradient of k_{on} and an intercept of k_{off}.

To apply this analysis to our data, we first fitted the acoustically detected real-time binding curves of the His-tagged fragment at each concentration to a single-exponential curve, as shown in Figure 5a. This fit was then used in the subsequent kinetic analysis. The plot of $\Delta(dR/dt)/\Delta R$ against C_{Ab} is shown in Figure 5b. A straight line fit to the data gives $k_{off} = 1.3 \times 10^{-3}$ s^{-1} and $k_{on} = 2.56 \times 10^4$ M^{-1} s^{-1}. We thus obtain the apparent binding constant, $k_{eq} = 1.97 \times 10^7$ M^{-1} for the histidine/Ni^{2+} binding. The fact that there is such a good agreement between the equilibrium constant calculated from the real-time analysis and that calculated from the binding isotherm indicates that the total phase change measured on addition of each concentration of antibody corresponded to a stage very close to equilibrium.[27]

Finally, it is worth mentioning that in our flow setup, the generation of turbulent flow near the entrance region of the flow chamber promotes good mixing, and the system is not mass-transfer-limited; for this reason, it is possible to calculate the kinetic constants of the interaction from the real-time graphs. More information on the specific design of the flow cell and the calculation of the mass transfer rates can be found elsewhere in the literature.[27]

Specificity and Reversibility of the Binding. For sensing applications, the development of a reversible biorecognition surface that binds specifically the analyte of interest is extremely important. In this application, the specificity of the binding was investigated under various conditions. Zero phase change was detected during the application of the His-tagged protein to a surface not exposed to nickel; similar response was observed when proteins without a His tag (BSA, IgG) were exposed to the nickel-bound bilayer. In addition, two different washing procedures were applied to regenerate the surface; the supported lipid bilayer and silica surfaces were regenerated after washing with EDTA or strong detergents, respectively (Figure 6). Histidine or imidazole can also be used as eluting agents instead of EDTA.

CONCLUSIONS

The attractive features of the method described above are that a metal-chelating supported bilayer can be easily produced on a hydrophilic surface, such as silica, by vesicle fusion in a single step and by using readily available chemicals. In contrast to other methods reported so far, this preparation procedure involves no laborious synthetic chemistry steps and provides a general approach to the specific and reversible immobilization of His-tagged proteins. Such a biorecognition layer can be further used in combination with any suitable surface-sensitive technique for further studies. In this work, the high-frequency surface acoustic waveguide biosensor was used as the main detection platform. It was shown that the kinetics of the vesicle fusion, as this was

(27) Saha, K.; Bender, F.; Gizeli, E. *Anal. Chem.* **2003**, *75*, 835−842.

monitored with the acoustic wave device, provides a reliable way to evaluate in situ the type of lipid layer formed and ensure that a lipid bilayer has been deposited on the device surface instead of a vesicle layer. Furthermore, real-time acoustic curves obtained during the binding of a His-tagged antibody fragment to the nickel-chelating SLB were used to derive information on the kinetic and equilibrium constants of the interaction.

The described surface modification method could find significant applications in areas such as proteomics, drug screening, biosensors, and the development of planar bilayers in an array format, whereas the acoustic waveguide device can provide an attractive alternative to direct optical techniques.

ACKNOWLEDGMENT

The authors acknowledge Dr. K. Melzak for fruitful discussions and Dr. A. Flewitt for his technical assistance in depositing the silica layer.

Received for review July 26, 2003. Accepted February 2, 2004.

AC034855G